

Laser Optical Interferometry in Electrochemistry and Corrosion: Fundamentals and Applications

K. Habib*, K. Al-Muhana, and A. Habib

*Materials Science Lab, Department of Advanced Systems

K I S R, P. O. Box 24885 SAFAT 13109 Kuwait

Tel:965-5430238, Fax:965-5430239, E-mail:khaledhabib@usa.net

ABSTRACT

In the present investigation, holographic interferometry was utilized for the first time to determine the rate change of the number of the fringe evolutions during the corrosion test of carbon steel in blank seawater and with seawater with different concentrations of a corrosion inhibitor. In other words, the anodic dissolution behaviors (corrosion) of the carbon steel were determined simultaneously by holographic interferometry, an electromagnetic method, and by the Electrochemical Impedance (E.I) spectroscopy, an electronic method. So, the abrupt rate change of the number of the fringe evolutions during corrosion test, (E.I) spectroscopy, of the carbon steel is called electrochemical emission-spectroscopy. The corrosion process of the steel samples was carried out in blank seawater and seawater with different concentrations, 5-20ppm, of RA-41 corrosion inhibitor using the E.I spectroscopy method, at room temperature. The electrochemical emission spectra of the carbon steel in different solutions represent a detail picture of the rate change of the anodic dissolution of the steel throughout the corrosion processes. Furthermore, the optical interferometry data of the carbon steel were compared to the data, which obtained from the E.I. spectroscopy. Consequently, holographic interferometric is found very useful for monitoring the anodic dissolution behaviors of metals, in which the number of the fringe evolutions of the steel samples can be determined in situ.

KEYWORDS :Optical interferometry, Corrosion, Corrosion inhibitor, Carbon steel, Electrochemical emission spectroscopy, Henry's Law and Seawater.

INTRODUCTION

In recent works conducted by the author^[1-16], an optical transducer was developed for materials testing and evaluation of different electrochemical phenomena. The optical transducer was developed based on incorporating methods of holographic interferometry for measuring microscopic deformations and electrochemical techniques for determining electrochemical parameters of samples in aqueous solutions. In addition, the optical transducer was applied not only as an electrometer for measuring different electrochemical parameters but also, the optical transducer was applied as a 3D-interferometric microscope for detecting different micro-alterations at a metal surface in aqueous solution, at a microscopic scale. Initially, the optical transducer was used to determine the mechanochemical behaviors of metals in aqueous solution, i.e., stress corrosion cracking, corrosion fatigue, and hydrogen embrittlement^[1-5]. The determination of the mechanochemical behaviors of metals in aqueous solutions, were based on detecting micro-deformations and measuring the corresponding current density by the optical transducer. Further more, the optical transducer was applied as an optical corrosion-meter^[6-8] for measuring cathodic deposit and anodic dissolution layers of metals in aqueous solutions. Also, the optical corrosion-meter was utilized to determine the cathodic and anodic current densities, which correspond to the cathodic deposit and anodic dissolution layers, respectively. The cathodic and anodic current densities were measured electromagnetically by the optical transducer, rather than electronically by one of the classical methods, i.e, an Ammeter, of measuring the

This is an unrefereed preprint, and it should not be referenced.
The refereed paper will appear in the Journal of Corrosion
Science and Engineering at <http://www.umist.ac.uk/corrosion/jcse>

This paper was presented at the Conference "Corrosion
Science in the 21st Century" held at UMIST in July 2003.

flow of the electronic current in a conductor. In addition, the optical transducer was applied to measure uniform corrosion and localized corrosion on metal surfaces and on substrates covered by organic coatings or under crevice assemblies^[8-14]. The optical transducer also, was used to document adsorption and desorption phenomena of chemical species on metal surfaces in aqueous solutions^[12]. Finally, the optical transducer was applied as an electrometer for measuring the double layer capacitance, the alternating current impedance and the corresponding oxide layer thickness of metals in aqueous solution^[15-17].

The objective of the present work was to determine the rate change of the number of the fringe evolutions during the corrosion test of a carbon steel in blank seawater and seawater with different concentrations of a corrosion inhibitor. In other words, the anodic dissolution behaviors (corrosion) of the carbon steel were determined simultaneously by holographic interferometry, an electromagnetic method, and by the Electrochemical Impedance spectroscopy (EIS)^[18], an electronic method. So, the abrupt rate change of the number of the fringe evolutions during corrosion test, (EIS), of the carbon steel is called electrochemical-emission interferometry.

THEORETICAL ANALYSIS

In a mathematical relationship derived by the author elsewhere^[7&8], one can measure the corrosion current density (J) of metallic samples in aqueous solutions according to the following mathematical model^[7&8]:

$$J = \frac{F |Z| DU}{MT} \quad (1)$$

Where J is the corrosion current density of the based metal.
F is Faraday's constant.
|Z| is the absolute number of electron charge.
M is the atomic weight of the sample material.
T is the time of the anodic current.
D is the density of the based metal.
U is the orthogonal displacement of metal surface due to corrosion, where

$$U = N \lambda / (\sin \alpha + \sin \beta) \quad (2)$$

Where

N is the number of fringes.
λ is the wavelength of the laser light used in the experiment.
α is the illumination angle.
β is the viewing angle, both α and β can be obtained from the set up of the experiment.

A details derivation of equation No.1 and equation No. 2 is given elsewhere in literature^[7&8].

Equation No.1 describes the relationship between the corrosion current density, J, and the orthogonal displacement of metal surface due to corrosion, U. In other words, one can measure the corrosion current density of the based metal by knowing the thickness of the orthogonal displacement of metal surface due to corrosion. Since the thickness of the orthogonal displacement, U, can be measured by holographic interferometry from equation No.2. Therefore, one can correlate the number of the fringe evolutions, N, to the corrosion current density, J.

By applying equation No.1, one can detect the electrochemical emission-spectroscopy of the carbon steel in the blank seawater and seawater with the addition of the corrosion inhibitor by holographic interferometry. This can be achieved by plotting dN Versus the elapsed time of the experiment, where dN is the difference between the number of the fringe evolutions of two subsequent readings of the number of fringe evolutions. By plotting dN versus time, this will definitely reflect the abrupt rate change, electrochemical emission-spectroscopy, of the anodic dissolution behaviors of the steel samples as a function time of the corrosion test.

EXPERIMENTAL WORK

Metallic samples of a carbon steel, UNS No. 1020, were used in this investigation. The chemical composition of the carbon steel is 0.18-0.23%C, 0.3-0.6%Mn, and Balanced Fe. The carbon steel samples were fabricated in a rectangular form with dimensions of 5cm X 10cm X 0.15cm. Then, all samples were covered by a black epoxy (polyamide tar) except one side of the samples. The reason behind covering the samples by the black epoxy is to isolate the surface area of the samples from contacting the seawater, while testing the bare side of the samples to corrosion in seawater. At the beginning of each test, the carbon steel sample was immersed in an aqueous solution for nearly 45minutes. While the sample was in the solution the corrosion potential was monitored by a potentiometer with respect to the Saturated Calomel Electrode (SCE), a reference electrode, until the steady state potential reached. The carbon steel samples were tested in blank seawater and seawater with an addition of 5-20 ppm RA-41 corrosion inhibitor. The Chemical composition of the blank is given in Table 1. The PH of the blank seawater, seawater with 5ppm RA-41, seawater with 10ppm RA-41, and seawater with 20ppm RA-41 is 8.24, 8.23, 8.22, and 8.2, respectively. Then, a hologram of the sample was recorded using an off axis holography, see Figure 1 for the optical set up. In this study, a camera with a thermoplastic film was used to facilitate recordings of the real time-holographic interferometry of the samples during the corrosion test. The camera is HC-300 Thermoplastic Recorder made by Newport Corporation. For more details on the procedures of the experiment, the reader is encouraged to refer to literature elsewhere^[7&8]. In the mean time, The alternating current(A.C)-impedance measurements were recorded simultaneously with the optical holographic measurements by using the same sample. The A.C-impedance measurements were conducted by using the ACM Gill 8AC impedance system. The obtained data of the A.C-impedance measurements were basically Nyquist plots^[18], plots of the real alternating current impedance (z') versus the imaginary alternating current impedance (z''). By using Nyquist plots, a number of electrochemical parameters of the carbon steel samples in different solutions of seawater can be determined. But the most significant parameter for this investigation is the polarization resistance of the carbon steel samples in different solutions of seawater. This is because from the polarization resistance values, the corrosion current density can be determined from the linear polarization method^[19]. For instance, Figure 2a,b represents EIS plots of the carbon steel in seawater with 10ppm of RA-41 inhibitor. Figure 2a and Figure 2b represent the complex plane (Nyquist) plot and Bode plot, respectively. The frequency range of the EIS (given in Figure 2a,b) was divided into three regions with time as the followings:
Interval 1- from 100000Hz to 13Hz, from 1 to 5 minutes.
Interval 2- from 13Hz to 0.0304 Hz, from 5 to 15 minutes.
Interval 3- from 0.0304 Hz to .001Hz, from 15 to 25 minutes.

In this investigation, from the obtained complex plane (Nyquist) plots, i.e., in Figure 2a, electrochemical parameters such as the polarization resistance, solution resistance, and double layer capacitance were obtained by using the semi circle fitting method^[18]. This can be achieved by selecting the best fitting for the semicircle on the complex plane (Nyquist) plot, by using a computer software on the ACM Gill 8AC impedance system. Electrochemical parameters obtained by the EIS measurements such as the polarization resistance, solution resistance, and double layer capacitance of the carbon steel sample tested in blank seawater and seawater with 5-20 ppm RA-41 inhibitor are given in Table 2.

It is worth mentioning that in each experiment, the holographic interferograms were recorded as a function of time, in which each test lasted for less than 30 minutes, the duration of the EIS measurement. Then, the difference between the number of the fringe evolutions of two subsequent numbers of the fringe evolutions, dN , were plotted as a function time in order to show the abrupt rate change of electrochemical-emission interferometry of the samples in different solutions. The abrupt rate change of electrochemical-emission interferometry was recorded each consecutive minute of the elapsed time the experiment.

RESULTS AND DISCUSSION

Figure 3a,b shows an example of progressive interferograms of a carbon steel sample in seawater with 5ppm RA-41 corrosion inhibitor as a function of time. Figure 3a represents a real-time interferogram of the sample after 1 minute of the elapsed time of the corrosion test, where 7 fringes appeared on the photograph. This indicates that the carbon steel sample has oxidized right away after the sample immersion in seawater. This behavior is well known

about the carbon steel in seawater^[20]. Figure 3b is the same interferogram after 3 minutes of elapsed time of the corrosion test, where 18 fringes detected on the photograph. It is obvious from this photograph that there is a general chemical oxidation, depicted by the uniform interferometric patterns. It is worth mentioning that each fringe in figure 3 (dark line) accounts to an orthogonal displacement equivalent to $0.3\mu\text{m}$ according to mathematical models reported elsewhere^[7&8]. In other words, holographic interferometry can be used as a powerful tool, interferometric microscope, in the field of electrochemistry.

By using data from interferograms such as those in Figure 3, one can develop a relationship between the difference of the number of the fringe evolutions of two subsequent fringe numbers and the elapsed time of the experiment. Figures 4-7 show plots of the difference between the number of the fringe evolutions of two subsequent fringe numbers and the elapsed time of the experiment of the carbon steel in the blank seawater, seawater with 5ppm RA-41, seawater with 10ppm RA-41, and seawater with 20ppm RA-41, respectively. From figures 4-7, it is ready to determine the abrupt rate change of electrochemical emission-spectroscopy of the carbon steel samples in different solutions. For instance, Figure 4 shows the rate change of the difference between the number of the fringe evolutions of carbon steel in the blank seawater. It obvious from Figure 4 that the rate change of electrochemical emission-spectroscopy of the carbon steel was observed to increase gradually from $dN=1$ fringe to $dN=13$ fringes per minute, from the beginning to the end of the test. This behavior of the electrochemical emission-spectroscopy of the carbon steel in blank seawater indicates that the corrosion rate of the steel samples was continuously increasing as a function of time. On the contrary to the observation of the electrochemical emission-spectroscopy of Figure 4, the electrochemical emission-spectroscopy of carbon steel samples in seawater with additions of the RA-41 inhibitor were different. Figure 5-7 show the electrochemical emission-spectroscopy of carbon steel samples in seawater with 5ppm, 10ppm, and 20ppm of the RA-41 inhibitor, respectively. It is clear from figures 5,6, and 7, that the rate change of the number of the fringe evolutions was observed to vary between $dN=2-8$, $dN=1-5$, and $dN=0-3$ (steady state ranges), respectively. This behavior of the electrochemical emission-spectroscopy of the carbon steel in figures 5,6, and 7 indicates that the corrosion rate of the steel samples was in general decreasing as a function of the addition of the RA-41 corrosion inhibitor. In other words, the addition of 5ppm RA-41 to the seawater is found less effective inhibitor amount to protect the carbon steel from the seawater corrosion than the 10ppm and 20 ppm additions to the seawater. In fact the addition of 20 ppm of RA-41 is found the most effective inhibitor amounts than the rest addition of RA-41 amount to the seawater. But, in general, the difference between the number of the fringe evolutions of carbon steel among figures 5,6, and 7 is considered small (6,4, and 2 fringes), respectively as compared to the difference between the number of the fringe evolutions of carbon steel between figure 4 and figures 5,6, and 7, (10 fringes). This difference is due to the inhibition effect of the addition of RA-41 inhibitor on the corrosion behavior of the carbon steel in seawater. Furthermore, several abrupt changes of the electrochemical emission-spectroscopy were recorded in Figures 5,6, and 7, from the steady state values. For instance, two abrupt changes were observed in figure 5, at 4 minutes and 13 minutes, and in figure 6, at 4 minutes and at 20 minutes. In contrast, only one abrupt change was observed in figure 7, at 24 minutes. For the sake of the comparison between measurements of the electrochemical emission-spectroscopy (By holographic interferometry) and the E.I. spectroscopy (electronic measurement), the corrosion current density of the same carbon steel sample in blank seawater, seawater with 5ppm, seawater with 10ppm, and seawater with 20 ppm of RA-41 was determined $J=0.138\text{ mA/cm}^2$, $J=0.0229\text{ mA/cm}^2$, $J=0.0283\text{ mA/cm}^2$, $J=0.0175\text{ mA/cm}^2$, respectively, by the A.C. impedance measurements. It is obvious that there is an agreement between measurements of the electrochemical behaviors of the carbon steel samples in blank seawater, seawater with 10ppm, and seawater with 20 ppm of RA-41 by both methods, the electrochemical emission-spectroscopy (By holographic interferometry) and the E.I. spectroscopy (electronic measurement). In other words, the high value of the corrosion current density, $J=0.138\text{ mA/cm}^2$, of the carbon steel sample in blank seawater corresponds very well with the high rate change of the number of fringe evolutions, $dN=13$, which observed in Figure 4. In addition, the low value of the corrosion current density of carbon steel sample in seawater with 20ppm ($J=0.0175\text{ mA/cm}^2$) of RA-41 corrosion inhibitor corresponds very well with the low rate change of the number of fringe evolutions, $dN=3$, which observed in Figure 7. In fact the observations in this investigation agree very well with the Henry's law^[21] for dilute solution, in which the corrosion current density, J , and the difference of the rate change of the number of fringe evolutions, dN , of carbon steel samples were observed to decrease in a proportional linear manner with respect to the addition the RA-41 corrosion inhibitor to the seawater.

The obtained data of the corrosion inhibitor concentration, dN and J , are given in Table3. It is obvious from Table 3 that the concentration of inhibitor has a direct effect on both the current corrosion densities (J), which were measured by the E.I. spectroscopy method, and the rate of fringe evolution (dN), which were measured through the

optical method. By plotting the inverse values of the corrosion inhibitor concentrations versus the rate change of fringe evolution (dN) and current density (J), the “Henry’s constant”^[21] can be determined.

In Figure 8 a clear relationship is shown between the inverse values of the corrosion inhibitor concentration and the rate change of fringe evolution. The rate change of fringe evolution is found to increase in a linear manner to the decreasing concentration RA-41 (which is depicted in the graph as the increasing inverse concentration of RA-41) in accordance to Henry’s Law^[21]. The resulting function is $dN = 20 (1/C) + 2$; where the Henry Constant is $K' = 20$ dN/ppm. In figure 9, the corrosion current density is found to relate in a nonlinear manner with the inverse values of the concentration of the corrosion inhibitor. Although the corrosion current density was observed to increase from 0.0175 mA/cm² (at 20 ppm) to 0.0283 mA/cm² at 10 ppm; afterwards it was observed to decrease to 0.0229 mA/cm² at 5 ppm. These observations are not in agreement to Henry’s Law. Therefore it can be concluded that the optical method of holographic interferometry represents a sensitive tool of analytical electrochemistry, as compared to the E.I Spectroscopy method. This optical technique then allows an inside detail of the data analysis to be achieved leading to the determination of an analytical formula based on a known phenomenon of an ideal dilute solution (i.e. Henry’s Law). From obtained formula, subsequent dN values can be determined analytically for low concentrations of RA-41.

REFERENCES

1. K.Habib, *Applied Optics*, **29** (13), pp.867-869 (1990).
2. K.Habib, *Experimental Techniques of Physics*, **38** (5/6), pp. 535-538 (1990).
3. K.Habib, G.Carmichael, R.Lakes, W.Stwalley, *Corrosion Journal*, **49** (5), pp.354-362 (1993).
4. K.Habib, *Optics and Lasers in Engineering*, **20**, pp.81-85 (1994).
5. K.Habib, *Optics and Lasers in Engineering*, **23**, pp.65-70 (1995).
6. K.Habib, *Proc. SPIE*, **1230**, pp. 293-296 (1990).
7. K.Habib, *Optics and Lasers in Engineering*, **18**, , pp.115-20 (1993).
8. K.Habib, F.Al Sabti, and M.Al- Mazeedi, *Optics and Lasers in Engineering*, Vol.**27**, No.2, PP.227-233 (1997).
9. K.Habib, *Optics and Lasers in Engineering*, Vol.**23**, No.2, PP.213-219 (1995).
10. K.Habib and F.Al Sabti, *OPTICAL REVIEW*, Vol.**4**, No.2, PP.324-328 (1997).
11. K.Habib, and F. Al-Sabti, *Corrosion Journal*, **53**, (9) PP. 680-685 (1997).
12. K.Habib, *ELECTROCHEMICA Acta*, Vol. **44**, PP.4635-4641 (1999).
13. K.Habib, *Corrosion Science*, **40**, (8) PP. 1435-1440 (1998).
14. K.Habib, *Optics and Lasers in Engineering*, Vol.**31**, PP.13-20 (1999).
15. K.Habib, *Optics and Laser Technology*, Vol.**28**, No.8, PP.579-584 (1996).
16. K.Habib, *Optics and Lasers in Engineering*, Vol.**28**, PP.37-46 (1997).
17. K.Habib, *Corrosion Science*, Vol.43, No.3, PP.449-455 (2001).
18. “Basic of A.C.Impedance Measurements, application note-AC-1”, EG and G Princeton Applied Research, Electrochemical Instrument Division, Princeton, New Jersey, 1982.
19. R.Baboian, “Electrochemical techniques for Corrosion”, P.58, NACE Press, Houston, TX, 1977.

20.H.Uhlig, “Corrosions Corrosion Control”, PP.322-350, John Wiley & Sons Inc., New York, 1971.

21. Chang R., Chemistry, PP.477-478, 7th Edition, McGraw Hill, New York, (2002).

Table1 : Chemical composition of the blank seawater

Parameter	Maximum (ppm)	Minimum (ppm)	Normal Seawater (ppm)
Sodium	12433	11536	11860
Magnesium	1543	1490	1340
Potassium	459	469	410
Calcium	404	378	515
Copper	0.05	< 0.05	—
Zinc	0.05	< 0.05	—
Iron	0.5	<0.05	—
Manganese	0.1	<0.05	—
Chloride	22014	21933	20959
Sulfate	3272	3200	2650
Bicarbonate	161	156	130
Ammonia	1.13	0.02	—
Nitrate	0.025	0.002	—
Sulfide	0.2	0.005	—
Total Organic	8	8	—
Carbon	—	—	—
Total HC	0.327	0.204	—
Silica	0.09	0.05	—
TDS	46300	44100	35840
Bromide	80	—	66
Floride	1.25	—	1.3

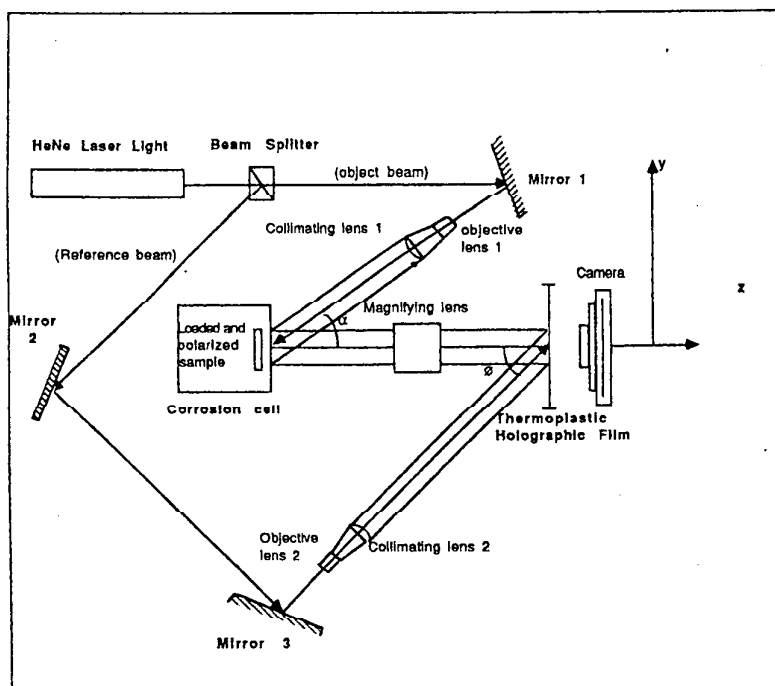
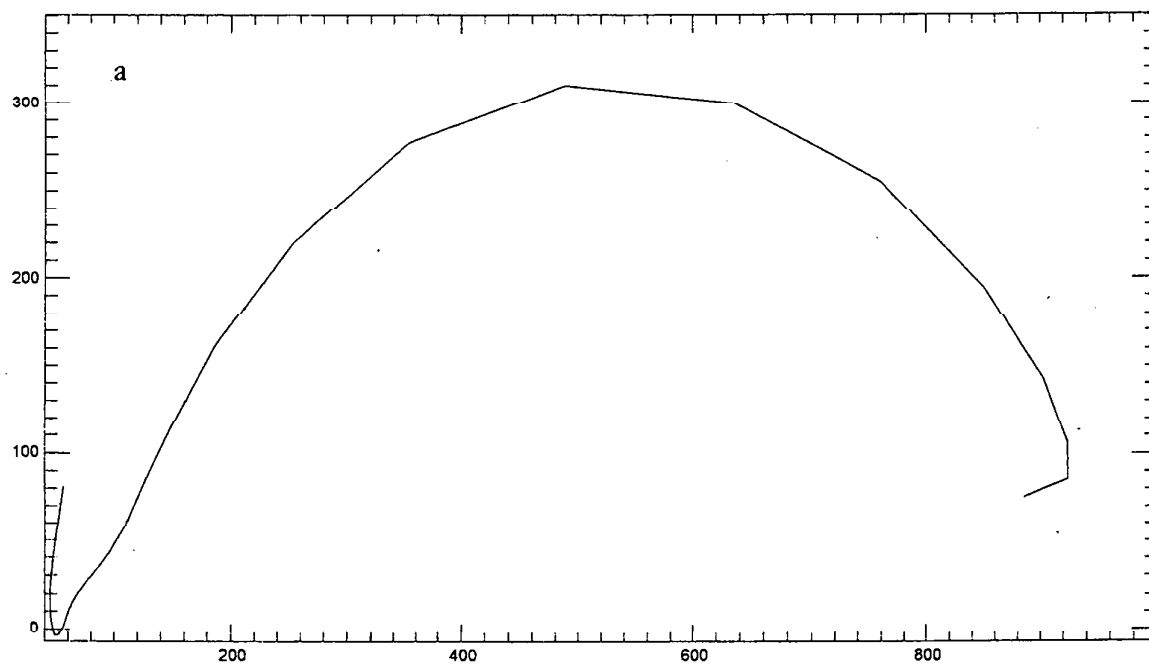


Fig.1. Optical setup of an off axis holographic interferometry.

Table 2: Electrochemical parameters obtained by EIS measurements of the carbon steel in the Blank Seawater and in the different inhibited solutions.

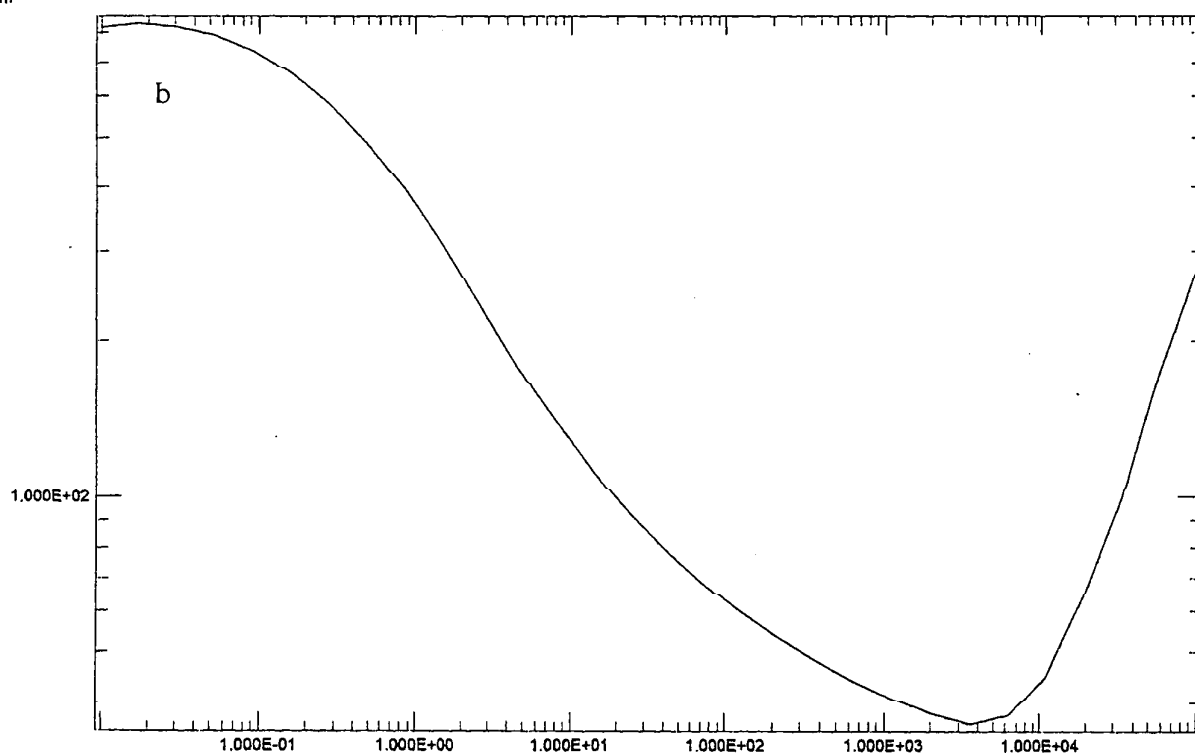
	Solution Resistance (Ωcm^2)	Polarization Resistance (Ωcm^2)	Double Layer Capacitance (Farad)
Blank Seawater	76.2	188.7	0.000281
Blank Seawater with 5ppm RA-41	67.6	1138	0.00472
Blank Seawater with 10ppm RA-41	82	930.4	0.00082
Blank Seawater with 20ppm RA-41	116	1488	0.0006

Z'' Ohms.cm²



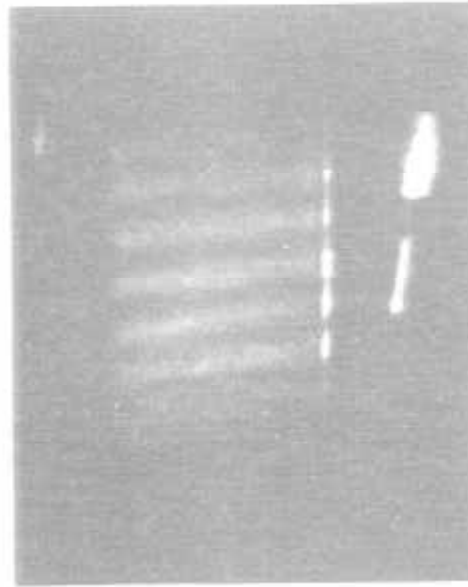
Z' Ohms.cm²

Ohms.cm²



Frequency (Hz)

Fig. 2a,b EIS plots for the carbon steel sample in seawater with 10ppm RA-41. Fig.2a represents the complex plane (Nyquist) plot and Fig.2b represents the Bode plot.



a



b

Fig. 3. Progressive interferograms of a carbon steel sample in seawater with 5ppm RA-41 corrosion inhibitor as a function of time: (a) after 1 minute, (b) after 3 minutes.

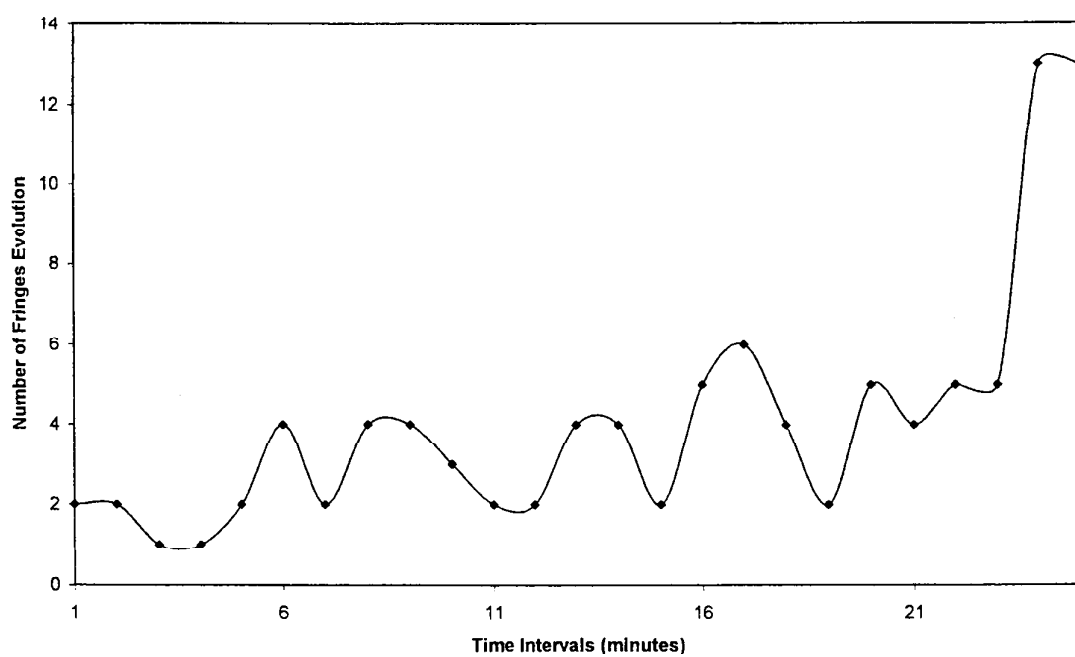


Fig.4. The Electrochemical emission-spectra of the carbon steel in blank seawater as a function of the elapsed time of the experiment .

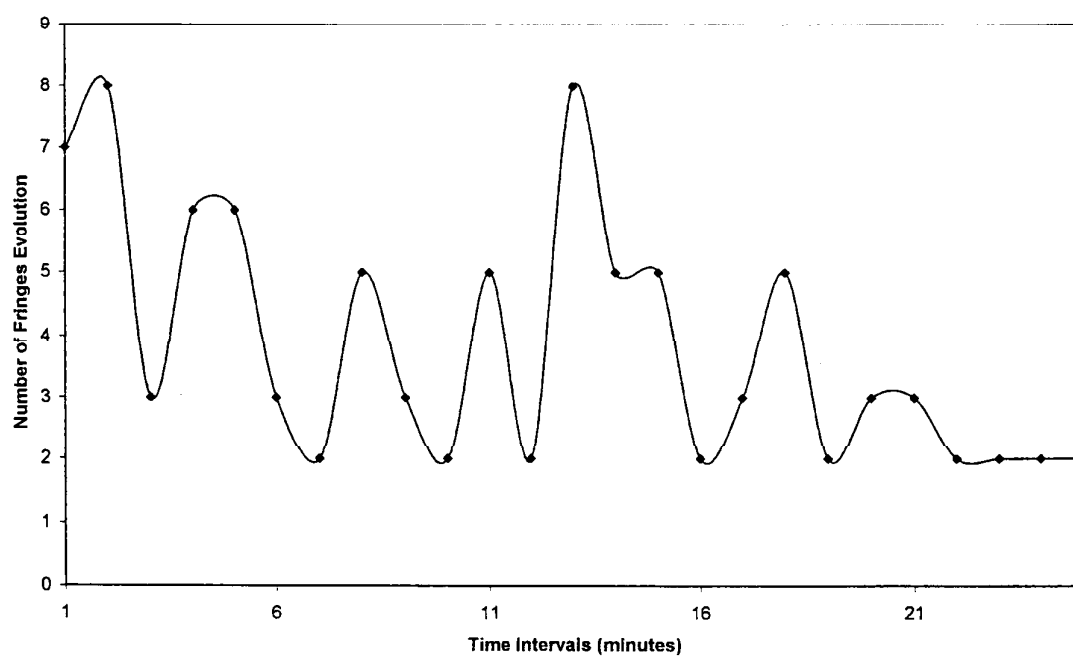


Fig.5. The Electrochemical emission-spectra of the carbon steel in seawater with 5ppm AR-41 as a function of the elapsed time of the experiment.

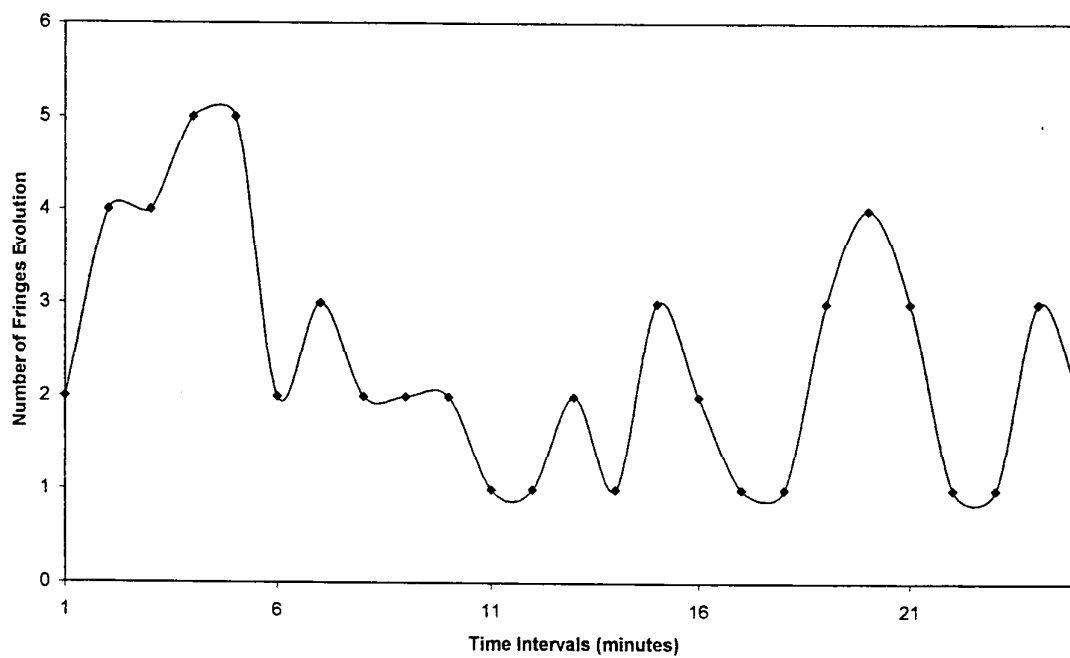


Fig.6. The Electrochemical emission-spectra of the carbon steel in seawater with 10ppm RA-41 as a function of the elapsed time of the experiment.

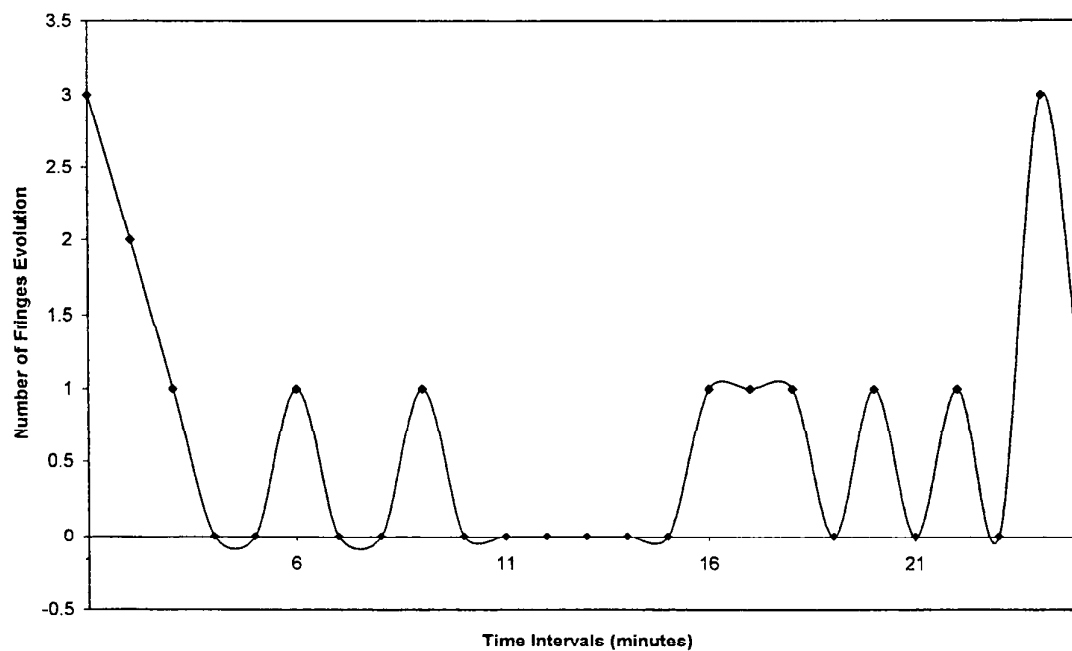


Fig.7. The Electrochemical emission-spectra of the carbon steel in seawater with 20ppm RA-41 as a function of the elapsed time of the experiment.

Table 3: The obtained data of the corrosion inhibitor concentration: dN and J.

RA-41 (ppm)	dN	J (mA/cm ²)
0	12	0.138
5	6	0.0229
10	4	0.0283
20	3	0.0175

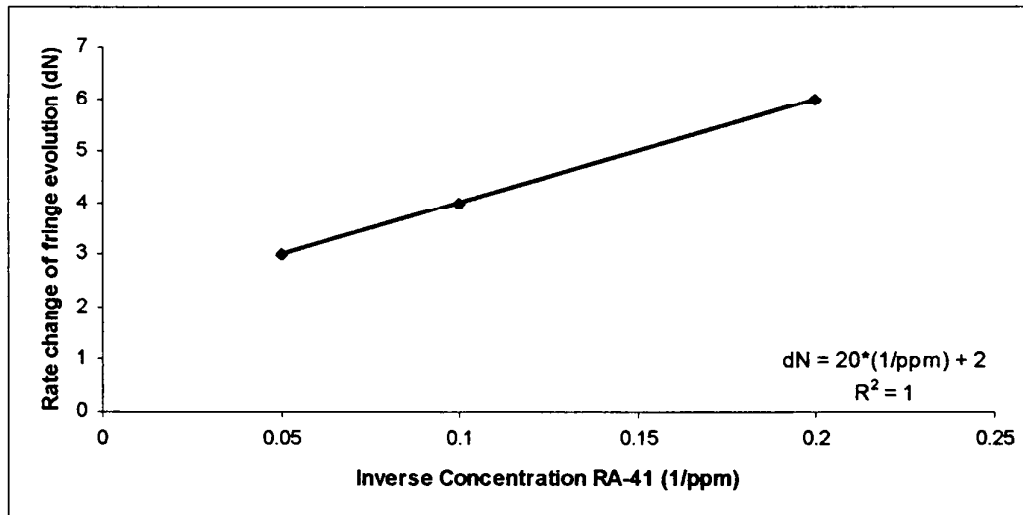


Fig.8. The relationship between the inverse values of the corrosion inhibitor concentration and the rate change of fringe evolution.

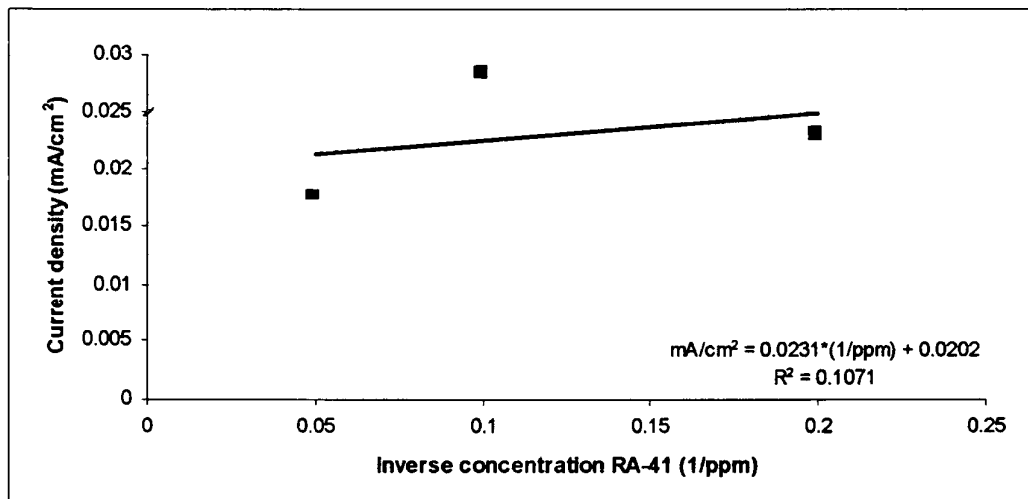


Fig.9. The relationship between the inverse values of the corrosion inhibitor concentration and corrosion current density.